# Nanoparticles in 472 Human Cerebrospinal Fluid: Changes in Extracellular Vesicle Concentration and miR-21 Expression as a Biomarker for Leptomeningeal metastasis

**Kyue-Yim Lee**
National CancerCenter
**Ji Hye Im**
National Cancer Center
**Weiwei Lin**
National Cancer Center
**Ho-Shin Gwak** ( nsghs@ncc.re.kr )
**Jong Heon Kim**
National Cancer Center
**Byong Chul Yoo**
National Cancer Center
**Tae Hoon Kim**
National Cancer Center
**Jong Bae Park**
National Cancer Center
**Hyeon Jin Park**
National Cancer Center
**Ho-Jin Kim**
National Cancer Center
**Ji-Woong Kwon**
National Cancer Center
**Sang Hoon Shin**
National Cancer Center
**Heon Yoo**
National Cancer Center
**Changjin Lee**
Rosetta Exosome Inc.

**Research**

**Keywords:** biomarker, cerebrospinal fluid, extracellular vesicle, microRNA, leptomeningeal metastasis

**Posted Date:** August 5th, 2020

**DOI:** https://doi.org/10.21203/rs.3.rs-52125/v1

**Version of Record:** A version of this preprint was published at Cancers on September 24th, 2020. See the published version at https://doi.org/10.3390/cancers12102745.

# Abstract

**Background:** Leptomeningeal metastasis (LM) has a poor prognosis and is difficult to diagnose and predict the response of treatment. In this study, we suggest that the monitoring of changes in the concentration of extracellular vesicles in cerebrospinal fluid could help to diagnose or predict outcomes for LM.

**Methods:** We measured nanoparticles in 472 human CSF from controls and patients including LM with both Dynamic Light Scattering (DLS) and Nanoparticle Tracking Analysis (NTA) after two-step centrifugations.

**Results:** NTA revealed nanoparticles distributed at a median 193 nm in size, and $1.74 \times 10^8$ /ml in concentration, and those were significantly higher in LM compared to other groups (211 nm vs. 188 nm, $p < 0.001$ and $2.80 \times 10^8$ /ml vs. $1.49 \times 10^8$ /ml, $p < 0.01$, respectively). Changes in NTA-measured nanoparticles (EV from here) concentration after intra-CSF chemotherapy were further examined in non-small cell lung cancer patients with LM ($n$=33). Overall survival was longer for patients with increased EV than the others (442 vs. 165 days, $p < 0.001$). Exosome surface markers (CD9/CD63/CD81) significantly decreased in the EV-decreased group (ratio 0.64, $p$<0.0001). MicroRNA-21 expression decreased in this favorable prognostic group, whereas increased in the EV-decreased group ($p = 0.003$).

**Conclusions:** The elevated concentration of extracellular vesicles in cerebrospinal fluid in patients with LM can be a diagnostic marker. Moreover, EV changes combined with microRNA-21 might be a biomarker for monitoring intracranial chemotherapy of LM.


# Introduction

Cerebrospinal fluid (CSF) bathes the central nervous system (CNS) as it circulates the whole neuraxis and transports neurotransmitters, bioactive substances such as hormones, and other actively or passively secreted molecules from brain cells [1]. Thus, researchers have sought to detect CNS disease activity by analyzing CSF [2–4]. Recent studies have examined nanoparticles in human biofluids and their role in normal physiology and disease processes [5, 6]. In particular, exosomes (30–200 nm) are one of the most abundant nanoparticles in biofluids [7, 8]. Human CSF has been studied to be rich in nanoparticles including extracellular vesicles (EVs) and extracellular RNAs. In the early 2010s, human CSF was discovered to contain EVs including exosomes and other biomaterials such as extracellular RNAs [7–9]. However, due to low level of these materials and a hardship to acquire CSF samples, not individual-based but mostly pooled CSF sample studies were performed [10–12].

Leptomeningeal metastasis (LM) is a terminal-stage cancer that is devastating to patients, with cancer cells spreading through the CSF and adhering to the entire CNS. The overall survival of LM patients is approximately 6–8 weeks, and there is no definitive treatment for LM except intra-CSF chemotherapy, which has a questionable cost/benefit profile due to both low response rate and neurotoxicity [13, 14]. Thus, early diagnosis is needed to challenge this formidable disease. However, a cytology-based diagnosis of LM has a 40–50% false negative rate due to the paucity of floating cancer cells within a small volume (< 5 ml) of CSF sample [15, 16]. Moreover, unlike other metastatic cancers, LM has no solid biomarker to monitor disease progression or treatment response, as cancer cells present not as a mass but in a sheet-like linear nodular pattern on neuroimaging,[17] and cytology-negative conversion is either rarely achieved or uncorrelated with prognosis [18–20].

There have been several studies to establish these nanoparticles as a biomarker for CNS tumors, but yet to be established mainly due to lack of general existence, reference values from many samples, and difficulty in setting standard method to measure quantitatively. Here, we measured nanoparticles in human CSF from 472 controls and patients with various CNS diseases to provide a reference value and to testify nanoparticles as a biomarker for LM diagnosis and treatment response monitoring. We also tracked changes in EVs concentration in CSF from LM patients

after intraventricular chemotherapy and analyzed its relationship with overall survival. Furthermore, we measured expression of a well-known onco-miRNA, miR-21, in CSF from non-small cell lung cancer patients with LM after intraventricular chemotherapy.

## Materials And Methods

# Patients and control groups

This observational study was approved by the Institutional Review Board of the National Cancer Center (NCC-150002, NCC-2014-0135), followed all rules and regulations regarding the protection of human subjects in clinical research, and in accordance with the ethical guidelines outlined in the Declaration of Helsinki. All patients were signed informed consent. For patients below 18 years, the informed consent was also obtained from a parent and/or legal guardian. We analyzed CSF samples from six groups of patients. Control groups without CNS tumors were composed of patients with systemic cancer (cancer control, CC) and patients without any cancer (healthy control, HC). The second category of patients was LM from systemic cancer. The third group of patients was having parenchymal brain metastasis but no LM (brain metastasis, BM). The 4th group of patients was with primary brain tumors other than brain metastasis (brain tumor, BT). The last group of patients was from various CNS diseases but no cancer (other disease, OD). To include CC, recent imaging (e.g., computed tomography, positron emission tomography) or bone marrow reports were evaluated to detect cancerous lesions. All LM patients were cytologically diagnosed and had positive neuroimaging studies (i.e., gadolinium-enhanced brain or whole-spine magnetic resonance imaging)[15].

# CSF preparation

CSF samples were obtained after Institutional Review Board approval of the National Cancer Center (NCC-150002) for the purpose of identifying CSF biomarkers. CSF samples were obtained via lumbar puncture during spinal anesthesia (CC), CSF cytology examination (LM, BM and BT), or CSF chemistry (OD). Other CSF samples were obtained from the cisternal/subarachnoid space during craniotomy (HC, BM and BT). CSF was centrifuged within 1 h at 1,500 g for 20 min for cell down at room temperature as storage in refrigerator (4 °C) increased nanoparticle concentration (supplementary Fig. 1A). The remainder of the samples was centrifuged again at 10,000 g for 30 min (cell debris removal) and kept frozen at -80ºC for genomic profiling and nanoparticle evaluation.

# Measurement of nanoparticles by Dynamic Light Scattering (DLS)

CSF (40 µl) was placed in a disposable cuvette for Zetasizer Nano measurement following the manufacturer's protocol (Malvern, Worcestershire, UK). The Zetasizer Nano system determines particle sizes (0.3 nm to 10 µm) by measuring their Brownian motion in the sample using dynamic light scattering. Of the measurement display modes, intensity particle size distribution (PSD) was chosen to represent the relative proportion (%) of nano-sized particles.

# Quantitative measurement of nanoparticles by Nanoparticle Tracking Analysis (NTA)

Pure CSF samples without dilution or concentration were used for quantitative measurement of EV-sized particles using the NanoSight instrument (Model NTA NS300 with 642 nm red laser module, Malvern, Worcestershire, UK), which is a laser-based light scattering system that provides general nanoparticle characterization in terms of size and concentration ($10^6$ to $10^9$ particles/ml). Pure CSF samples were loaded into the laser module sample chamber manually with a confirmation of no air bubbles, and an automated camera module tracked the Brownian motion of particles in the liquid sample. The in-built software (NTA 3.2, Dev. Build 3.2.16) calculated the EV size and concentration of triplicate of each sample with 30 seconds video capture. For the consistency of observed value, we used the sCMOS camera type

and fixed camera level at 8 of 10, and set the temperature at 25 °C. When the concentration was more than $10^9$ particles/ml, the sample was diluted and the initial concentration was calculated according to the dilution factor.

# Exosome fractionation by Exo-spin

To separate EVs from proteins, nucleic acids, and precipitating agents, the exosome suspension was fractionated using Exo-spin midi-columns (Cell Guidance Systems, St. Louis, MO) according to the manufacturer's instructions. Briefly, CSF was incubated with 500 µl Buffer A for 1 h at room temperature and then centrifuged for 1 h at 16,000 g. The exosome-containing pellet was suspended in 100 µl PBS. The exosome suspension was placed in the top of the column, and the eluate was discarded. The exosome-containing fraction was obtained in 200 µl PBS, and proportion changes were evaluated using Zetasizer Nano analysis.

# CSF concentration and Western blotting

15 ml of pre-centrifuged CSF was concentrated with Amicon® Ultra 15 mL Filter (Merck, Darmstadt, Germany), and 0.2 ml of concentrate was recovered. The concentrate was measured for protein concentration using a BCA protein assay kit (Pierce Biotechnology, Rockford, IL). The concentrate were resolved by 10% or 15% SDS-PAGE, transferred onto nitrocellulose membrane, blocked with 5% nonfat dry milk in TBST (10 mM Tris-HCl pH 7.5, 100 mM NaCl, and 0.05% Tween 20) followed by incubation with primary antibodies against exosome membrane CD63 or CD81 (Santa Cruz Biotechnology, Dallas, TX) or cytosolic protein cytochrome C or GM130 (BD Pharmingen, San Diego, CA). Blots were washed and incubated with HRP-conjugated secondary antibody. Antibody complexes were visualized using an enhanced chemo-luminescence Western blotting detection system (Pierce Biotechnology, Rockford, IL).

# Intact exosome isolation for transmission electron microscopy

Exosomes in clarified CSF were isolated using the ExoLutE exosome isolation kit (Rosetta Exosome Inc., Gyeonggi-do, Republic of Korea) according to manufacturer instructions. Briefly, thawed CSF samples were pre-filtered by 0.45 µm syringe filter (Millex→, Merck, Darmstadt, Germany) to remove debris and protein aggregates. Clarified CSF were further concentrated with 100 kDa MWCO centrifugal ultrafiltration device (Amicon, Merck, Darmstadt, Germany). Intact forms of exosomes in 8 mL concentrated CSF were purified by a method comprises exosome precipitation with metal-affinity and further purification with a spin-based size-exclusion chromatography. The purified CSF exosomes were subsequently subjected on transmission electron microscopy to determine their shapes and ultrastructures. 5 µL of exosome preparation at $1{\cdot}10^9$ particles /µL were adsorbed onto glow-discharged carbon-coated copper grids (Electron Microscopy Sciences, Hatfield, PA) for 5 min. After excess liquid removal, the grid was washed 10 times with PBS and subsequently stained with 2% uranyl acetate (Ted Pella, Redding, CA). The grid was finally examined in JEM 1011 microscope (JEOL, Tokyo, Japan) and images were recorded with an ES1000W Erlangshen CCD Camera (Gatan Inc. Pleasanton, CA).

# Extracellular RNA extraction from CSF

We used mirVana PARIS (Ambion, Mulgrave, Victoria, Australia) to extract extracellular RNA from cleared CSF according to the manufacturer's instructions. Briefly, 0.5 ml CSF was gently mixed with 2 × denaturing solution, acid-phenol:chloroform was added, and the mixture was centrifuged at 10,000 g for 5 min to separate the aqueous phase. After phase separation, a 1.25 volume of 100% ethanol was added to the aqueous phase, and the solution was loaded into the column and centrifuged at 12,000 g for 30 s. Extracted RNA was washed and eluted with 25 µl (95 °C) RNase-free water. The purity (A230/280 ratio) and concentration of dissolved RNA samples were measured using a Nanodrop spectrophotometer (ThermoFisher Scientific).

# Quantitative measurement of Extracellular Vesicles (Evs)

# MACSPlex

CSF samples after two-step centrifugation were subjected to bead-based multiplex EV analysis by flow cytometry with MACSPlex Exosome Kit (cat. 130108813, human, Miltenyi Biotec, Gladbach, Germany) as a provided protocol [21]. Briefly, 0.5 mL of EV-containing CSF samples were processed as follows: Samples were added 0.5 ml of MACSPlex buffer (MPB), 15 ul of capture beads and 15 ul of detection reagent mixture (APC-conjugated anti-CD9, anti-CD63, and anti-CD81 antibodies) to, and incubated for overnight using an orbital shaker (450 rpm) protected from light. To wash the samples, 500 ul of MPB was added to each tube and centrifuged at 3000 g for 5 min and the supernatant were removed. After washing 3 times, samples were resuspended to 0.5 ml of MPB buffer and transferred to 5 ml round bottom tube (cat. 352235, BD Bioscience) and analyzed with a BD LSRfortessa™ (BD Biosciences, San Jose, CA). For setting up the instruments, the Exosome setup beads were used, and the flow cytometry data were analyzed using FlowJo software (v10). The median fluorescence intensity (MFI) values of APC for CD9, CD63 and CD81 bead populations were used to determine the expression of exosome markers.

# Exoview

Quantitative measurement of EVs were tested with ExoView Tetraspanin kits (NanoView Bioscience, Boston, MA) as previously decribed [22]. CSF was diluted in PBS with 0.05% Tween-20 (PBST) and incubated on the ExoView Tetraspanin Chip (EV-TC-TTS-01) placed in a sealed 24-well plate for overnight at room temperature. After washing with PBST three times, chips were incubated with ExoView Tetraspanin Labelling ABs (EV-TC-AB-01) that consist of anti-CD81 Alexa-555, anti-CD63 Alexa-488, and anti-CD9 Alexa-647. The antibodies were diluted 1:5000 in PBST with 2% BSA. The chips were incubated with 250 µL of the labelling solution for 2 h. The chips were then washed once in PBST, three times in PBS followed by a rinse in filtered DI water and dried. The chips were then imaged with the ExoView R100 reader (Nanoview Bioscience, Boston, MA) using the ExoScan 2.5.5 acquisition software. The data were then analysed using ExoViewer 2.5.0 with sizing thresholds set to 50 to 200 nm diameter.

# miRNA digital droplet polymerase chain reaction (ddPCR)

To evaluate differences in miRNA expression between LM and normal CSF samples, we measured the expression of hsa-miR-21-5p by ddPCR. Approximately 2 µl purified total RNA was reverse-transcribed into cDNA using a Taqman advanced miRNA cDNA Synthesis Kit (Applied Biosystems, Foster City, CA) according to the manufacturer's instructions. A total of 5.5 µl undiluted cDNA was mixed with 2 × ddPCR Supermix (Bio-Rad Laboratories, Inc., Hercules, CA) and Taqman advanced miRNA Assay probes (Applied Biosystems). Each PCR sample was partitioned into up to 20,000 nl-sized droplets by a Bio-Rad QX299 droplet generator. Forty µl of each PCR mixture underwent the following cycling protocol: 95 °C for 10 min (DNA polymerase activation), followed by 40 cycles of 94 °C for 30 s (denaturation) and 60 °C for 1 min (annealing), followed by post-cycling steps of 98 °C for 10 min (enzyme inactivation) and an infinite 4 °C hold. The amplified PCR product of the nucleic acid target in the droplets was quantified in the FAM channel using a QC200 Droplet Reader (Bio-Rad Laboratories, Inc.) and analyzed using QuantaSoft v.1.7.4.0917 software (Bio-Rad Laboratories, Inc.).

# Statistical analysis

Categorical data were analyzed using Chi-square, Fisher's exact, or Mann-Whitney U tests as appropriate. Continuous data were analyzed using Student's t-tests or analysis of variance (ANOVA) with Scheffe's tests for post hoc comparisons. A two-tailed $p$-value < 0.05 was considered statistically significant. Statistical analyses were performed using SPSS 18.0 (SPSS, Chicago, IL) or GraphPadPrism 6 (GraphPadPrism Software, La Jolla, CA).

## Results

# Patient characteristics

A total of 669 CSF samples consecutively obtained from six groups of patients between 2014 and 2019 were used for the analysis of nano-sized particle proportion. Preliminary analysis showed that the proportions of nano-sized particles changed after treatment in LM patients (Supplementary Fig. 1B). Hence, for this group of patients, 197 post-treatment samples were excluded and only pre-treatment samples were included in the comparative analysis between patients groups. Demographic characteristics of the 472 patients in the proportion analysis are summarized in Table 1 according to patient group. The median age of all patients was 48 years (range, 0.2–90 years). Non-small cell lung cancer (NSCLC) was the most frequent primary cancer type among LM and brain metastasis patients.

Table 1
Clinical characteristics of CSF sample analysis ($n$ = 472)

| Groups | Total | Cancer control ($n$ = 100) | Healthy control ($n$ = 73) | LM ($n$ = 150) | Brain metastasis ($n$ = 28) | Brain tumors ($n$ = 72) | Other disease of CNS ($n$ = 49) |
|---|---|---|---|---|---|---|---|
| Gender | | | | | | | |
| Male | 215 (45%) | 70 (70%) | 31 (43%) | 53 (36%) | 13 (46%) | 36 (50%) | 12 (25%) |
| Female | 257 (55%) | 30 (30%) | 42 (57%) | 97 (64%) | 15 (54%) | 36 (50%) | 37 (75%) |
| Median age (range) | 48 (0.2–90) | 17 (1.5–90) | 59 (20–80) | 52 (2.0–79) | 55 (7–79) | 17 (1.9–80) | 40 (0.2–83) |
| Combined disease (%) | | Leukemia (62)<br>Bladder ca. (8)<br>Bone tumor (7)<br>Lymphoma (4)<br>Breast ca. (3)<br>Colon ca. (3)<br>Prostate ca. (2)<br>Cholangioca. (2)<br>Melanoma (2)<br>Others (7) | Unruptured An. (43)<br>Moyamoya ds. (12)<br>Hydrocephalus (5)<br>ICA stenosis (4)<br>BPH (2)<br>Head trauma (2)<br>Fibromatosis (2)<br>Others (3) | NSCLC (64)<br>Breast ca. (35)<br>Glioma (15)<br>Non-glial BT (10)<br>SCLC (4)<br>Stomach ca. (4)<br>PCNSL (2)<br>MUO (2)<br>melanoma (2)<br>Others (16) | NSCLC (16)<br>Breast ca. (6)<br>HCC (1)<br>Melanoma (1)<br>Ovarian ca. (2)<br>Sarcoma (1)<br>SCLC (1) | Glioma (19)<br>Medulloblastoma (15)<br>Germ cell tumor (9)<br>Non-glial MBT (6)<br>Ependymoma (7)<br>Pituitary adenoma (6)<br>Other benign BT (6)<br>Neurinoma (4) | MS (25)<br>ICH (13)<br>Infection (9)<br>Other AID (2) |

Abbreviations: AID, autoimmune disease; An, aneurysm; BPH, benign prostate hypertrophy; BT, brain tumor; HCC, hepatocellular carcinoma; ICA, internal carotid artery; ICH, intracranial hemorrhage; LM, Leptomeningeal metastasis; MBT, malignant brain tumor; MS, multiple sclerosis; MUO, malignancy of unknown origin; NSCLC, non-small cell lung cancer; PCNSL, primary central nervous system lymphoma; SCLC, small cell lung cancer

[a]Numbers in parenthesis are vertical proportion.

# Nano-sized particle peaks in CSF observed by Dynamic Light Scattering (DLS)

Relative proportions of nanoparticles in CSF samples by DLS based on intensity particle size distribution (PSD) were obtained using Zetasizer Nano and built-in software. Although the Zetasizer Nano can detect PSD at the millimeter range, we deliberately abandoned peaks outside the nanometer range (> 1,000 nm) on the relative proportion calculation. Majority of the samples ($n$ = 373, 79%) exhibited two peaks of various PSD proportion (Fig. 1(A and B)). However, a single peak pattern ranging widely from 10 nm to 1,000 nm (8%) or the three peaks pattern (13%) showing the 2nd peak between 10 nm and 100 nm and the 3rd peak at 100–1,000 nm range were also observed. For samples that exhibited two peaks, the estimated sizes of CSF particles in the small and the large peaks were 10.5 nm (standard deviation (SD), 4.52) and 176 nm (SD, 179.6), respectively (Fig. 1(C and B)).

The proportions of nanoparticle peaks in CSF varied across individual patients and among patient groups. For samples that exhibited two peaks, the relative proportions of the small and the large peaks differed depending on patient group (Supplementary Fig. 2(A)). Compared with all other patient groups, LM patients exhibited a significantly lower small peak proportion (35% vs. 55%) and higher large peak proportion (64% vs. 44%, $p < 0.0001$). Upon further analysis, we found that the large peak was associated with a significantly larger particle size in LM patients than in the other patient groups (mean 252 vs. 188 nm, $p < 0.0001$; Supplementary Fig. 2B).

# Verification of exosomes in CSF

Based on previous studies [6, 7, 10], we assumed that EVs in CSF account for large nanoparticles observed in our CSF samples. To understand the type and origin of EVs, the expression level of several cellular markers was detected in concentrated CSF (Fig. 1(E)). CSF samples were free with cellular proteins such as GM130 and cytochrome c, indicating the EVs markers present in CSF were not originated with cells contaminating CSF samples. Instead, CD81 and CD63, markers of microvesicles, were clearly detected. We then isolated intact EVs from CSF samples to examine their morphology and sizes. Transmission electron microscopic analysis of EVs isolated from CSFs revealed that EVs in CSF exhibited typical shapes of membranous nanovesicles secreted from mammalian cells and their sizes were highly heterogeneous ranging from 50 to 200 nanometers in diameter (Fig. 1(F)).

As an indirect method, we observed that the use of a commercially available exosome purification kit that bases on the size exclusion chromatography technology and eliminates protein or nucleic acid from samples (Exo-spin™) nearly abolished the small peak and increased the proportion of the large peak in DLS measurement (Supplementary Fig. 3A and B).

# Differences in EV concentration and size in CSF measured by Nanoparticle Tracking Analysis (NTA)

We measured the nanoparticles (presumed to be ‘extracellular vesicles (EVs from here) concentration and size in samples of unaltered CSF (neither diluted nor concentrated) after two-step centrifugation from different patient groups by NTA using NanoSight NS300 at the same camera condition as described in the Methods (Fig. 2(A)).

The measured EVs concentration of 472 samples was a mean of $3.46 \times 10^8$ particles/ml (SD, $0.29 \times 10^8$) and different among patients groups (Fig. 2(B)). Healthy control patients (HC) exhibited the lowest EV concentration, with a mean of $2.22 \times 10^8$/ml ($\pm 159 \times 10^8$). Cancer control (CC) and brain metastasis (BM) patients exhibited mean EV concentrations of $2.68 \times 10^8$/ml ($\pm 6.41 \times 10^8$) and $2.49 \times 10^8$/ml ($\pm 3.15 \times 10^8$), respectively. LM patients exhibited the highest mean EV concentrations of $7.15 \times 10^8$/ml ($\pm 9.15 \times 10^8$), which was a significantly higher than all other groups ($p < 0.0001$) except other CNS disease group. Patients with other CNS diseases (OD) showed the widest distribution of EV concentrations. The OD group consisted of patients with autoimmune disease ($n$ = 25 out of 27 patients with multiple sclerosis), intracranial hemorrhage ($n$ = 13), or CNS infection ($n$ = 9). Patients with autoimmune disease exhibited a mean EV concentration of $1.31 \times 10^8$/ml ($\pm 1.33 \times 10^8$), whereas patients with intracranial hemorrhage or CNS infection exhibited

higher mean EV concentrations of $15.32 \times 10^8$/ml (± $24.15 \times 10^8$) and $14.86 \times 10^8$/ml (± $27.58 \times 10^8$), respectively (Supplementary Fig. 4A).

We also analyzed the size of EV measured by NTA according to patients groups. The mean EV size of LM group was significantly larger than other groups (Fig. 2C and supplementary table 1, ANOVA, $p < 0.001$). The mean EV size of the other CNS disease group was also significantly smaller than other groups ($p < 0.001$). In detail, the subgroup of intracranial hemorrhage and autoimmune disease (171 ± 36 nm and 175 ± 22 nm, respectively) drove the EV size of OD groups into the smallest (Supplementary Fig. 4B).

To compare relative EV size distribution between groups, empirical cumulative distribution function (ECDF) plots were generated. LM groups showed the largest distribution as depicted by ECDF plot (Fig. 2(D)), followed by OD group. As depicted on the ECDF plot, the heterogeneity of EV size depend on increase of large size EV in LM patients, whereas that of OD group came from the relatively small sized EVs. Also, we analyzed the proportion of EV size with an interval of 50 nm from 0 to 300 nm, which was tentative limitation of EV size range (Fig. 2(E)). The LM group showed significantly higher proportion of EV size more than 150 nm compared to BT and control groups ($p < 0.05$, Kruskal-Wallis test, Dunn's Multiple Comparison method). Meanwhile, the proportion of 50–150 nm sized EV was higher in BT and control groups than that of LM ($p < 0.05$).

We compared these values by NTA to those measured by DLS. In DLS measurement, we assumed the large peak to be EV-sized and calculated a mean of the large peak size by intensity PSD to be a mean EV size. The discrepancy of the mean values between DLS and NTA was various among patients groups (supplementary table 1).

# Verification of non-vesicular particles among NTA measured EV in CSF

Although protein level is relatively low in CSF compared to serum, it has been known that various lipoproteins could be observed at EV size range in human biofluids [23]. To identify protein aggregates in CSF nanoparticles, we treated CSF with proteinase K (2 ng/mL) incubated for 60 minutes at 37 °C. All samples showed the shift-to-left pattern of peaks above 250–300 nm, but the EV concentration after proteinase is varied (Supplementary Fig. 5(A, B)). Fourteen (64%) samples showed decreased EV concentration, whereas 6 samples (27%) revealed increased and 2 samples remain without discernible change (< 20%). HC and BM showed a mean EV concentration ratio (proteinase K treated/untreated) 0.98 (± 0.32) and 0.97 (± 0.70), respectively. However, LM groups revealed significantly decreased EV concentration ratio of 0.69 (± 0.28) (Supplementary Fig. 5C, *paired t-test*, $p < 0.05$).

# Change in EV concentration in LM patients after intraventricular chemotherapy

Among LM patients, 41 were enrolled in a prospective clinical trial (http://cris.nih.go.kr, Identifier: KCT0000082) of ventriculolumbar perfusion (VLP) chemotherapy with methotrexate [24]. Briefly, 24 mg methotrexate premixed with artificial CSF was continuously infused to the lateral ventricles, and lumbar drainage was used to drain the CSF at the same infusion rate by hydrostatic pressure for 3 consecutive days. Abide by the protocol, these patients had matched pre-treatment (day 0) and post-treatment (day 4) CSF samples, and we analyzed changes in EV concentration after intraventricular chemotherapy (Supplementary Fig. 6A). We found that EV concentration decreased in 25 patients (61%), did not change (< 20%) in five patients (12%), and increased in 11 patients (27%) (Supplementary Fig. 6B). We evaluated the relationship between treatment-induced change in EV concentration and overall survival. The median overall survival (OS) of patients with increased EV concentration was 342 days (95% confidence interval (CI), 172–512) and it was significantly prolonged to compared the patients with ‘no change (< 20% of EV concentration)’ (median 216 days, 95% CI, 117–315) and the patients with decreased EV concentration (median 119 days, 95% CI, 90–148) ($p = 0.037$,

Fig. 3(A)). Next, to eliminate from different primary cancer of various prognosis, we did subgroup analysis of 33 patients with the same primary cancer of NSCLC, adenocarcinoma. Median OS was 342 days (95% CI, 165–519) in patients with an increased EV concentration ($n = 10$) but it was only 170 days (95% CI, 97–242) in patients with 'no change' ($n = 4$) and 104 days (95% CI, 76–132) in patients with a decreased EV concentration ($n = 19$). The difference of OS was more significant in this subgroup analysis compared with that in all patients ($p < 0.001$, Fig. 3(B)). Taken together, we can assume that the change of CSF EV concentration (nanoparticle concentration measured by NTA) might be a prognostic biomarker in the LM patients who received the VLP with methotrexate treatment.

# Analysis of exosome surface markers among NTA measured EV in patients with LM receiving intraventricular chemotherapy

As we tentatively defined NTA measured nanoparticles to EVs in this study without exosome extraction process, we were inevitably included non-exosomal particles among EVs. Thus, we verified exosome concentration change using surface markers in selected (remained CSF is enough for further study) patients among those with increased and decreased EV concentration of the above survival analysis [24].

Beads bearing each of CD9/ CD63/ CD81 antibody capturing exosome in CSF were measured their mean fluorescence intensity (MFI) in patients with increased ($n = 10$) and decreased ($n = 19$) EV concentrations (Fig. 4(A and B)). MFI values of each sample were converted into a ratio of post-treatment to pre-treatment paired samples. In the decreased group, the EV markers were significantly reduced after intraventricular chemotherapy (ratio 0.64, $p < 0.001$), whereas increased groups showed no significant exosome concentration change (ratio 1.13).

We also verified these exosome changes further using ExoView Tetraspanin ChipTM in a limited number of CSF samples from the EV-increased and EV-decreased groups ($n = 3$ from each, Fig. 4(C and D)). A triplicate of each sample revealed that each exosome markers (anit-CD9/ CD63/ CD81) after the intraventricular chemotherapy were significantly decreased after the intraventricular chemotherapy (ratio of 0.58/ 0.53/ 0.47) in EV decreased group. Whereas the number of exosome markers were not significantly changed in EV increased group.

# Change in miRNA expression in patients with LM receiving intraventricular chemotherapy

As changes in EV concentration after the treatment were related to patients' OS, we next measured expression of a well-known onco-miRNA, miR-21, in NSCLC (adenocarcinoma). Among those above 33 patients with NSCLC, fourteen samples were available for this further analysis. The miR-21 expression measured by droplet digital polymerase chain reaction (ddPCR) (Supplementary Table 2) was normalized by EV concentration measured by NTA (Fig. 5). The miR-21 expression declined (> 0.2 fold change) in 4 out of 5 patients with an increased post-treatment EV concentration (mean fold change, 0.33; SD, 0.45) and was elevated in 5 of 6 patients with EV-decreased group (mean fold change, 17.90; SD, 30.7). Among the EV concentration 'no change' patients, one patient showed declined miR-21 expression and other 2 patients revealed no change of miR-21 expression (< 0.2 fold change) (mean fold change 0.64; SD 0.55). Together, no patients showed elevated miR-21 expression among 8 patients with 'no change' or EV-increased groups in contrast to 5/6 patients in EV-decreased group revealed elevated miR-21 expression. Thus, the probability of elevated miR-21 expression after the treatment was significantly higher in the EV-decreased CSF samples compared with the EV-increased or 'no change' ones (Fisher's exact test, $p < 0.005$).

# Discussion

# Nanoparticles in CSF

Because CSF is filtered from blood through the “blood-CSF barrier,” it contains clinically important biomolecules and extracellular vesicles of CNS disease [25, 26]. Our measurement of EVs by NTA showed different mean EV size according to different patients groups. The biggest mean EV size (211 nm) in LM samples might be due to a higher proportion of microvesicles and apoptotic bodies as compared with other groups as their relative proportion of large EV (> 150 nm) was higher in LM than other groups. Furthermore, LM groups showed significantly higher number of non-vesicular particles, which were measured by NTA as EVs (supplementary Fig. 4). Although we did not identify those particles abolished after proteinase K treatment, these non-vesicular particles were mainly at a size of more than 200 nm, and they can be a result of leptomeningeal disease activity, at which cancer cells destroy the surface membrane of brain and spinal cord.

# Differences in EV concentration in CSF among patient groups by NTA

The merit of our measurement of EV concentration by NTA is that we minimized sample manipulation and transfer before measurement (i.e., lipid membrane binding in high-resolution flow cytometry). Instead, we directly counted the number of EVs in clinically available CSF samples, requiring only two-step centrifugation to discard waste cells and debris. Our study proved that the EV concentrations of CSF is suitable for NTA measurement range $10^6$~$10^9$ particles/mL) without specific EV enrichment process and also, provided reference EV concentration for unaltered CSF from hundreds of patients with various CNS diseases. Counts of EVs in CSF by NTA can be varied by camera level and detection threshold [27]. However, we used the same NTA conditions for all our samples, although some patients with inflammatory disease exhibited more EVs than the recommended particle number per frame. Thus, the relative concentration of EVs could reflect a real difference in CSF environments between patients with different CNS diseases and can also change after treatment within individual patients.

Our observation of significantly higher EV concentrations in LM patients compared with other patients could be explained by the fact that the CSF of LM patients harbors many cells, including cancer cells and white blood cells, which is known to be a major source of secreted EVs [23]. Although many researchers have found more EV secretion from cancer cells in the form of oncogenic proteins (i.e., oncosomes) [28, 29], they did not measure differences in EV size between cancer and normal cells. We also could not determine whether the source of EVs was from floating cancer cells or white blood cells in this study. Among disease groups, the intracranial hemorrhage patients in other CNS disease group exhibited the highest EV concentration of mean $1.53 \times 10^9$ particles/ml followed by CNS infection. Spaull at al., who measured a EV concentration of unaltered CSF from preterm intracranial hemorrhage patients by NTA, reported $2.89 \times 10^{10}$ to $1.31 \times 10^{11}$ particles/ml in 3 samples[30]. Considering brisk hemorrhage in their CSF whereas our samples are not, these concentrations are comparable to each other.

# Change in EV concentration and miR-21 expression in LM patients after intra-CSF chemotherapy

Our observation of changes in EV concentration after the chemotherapy demonstrates the possibility of conveniently analyzing patient CSF samples by commercially available NTA to provide a useful biomarker of LM treatment response. In general, increased EV secretion could reflect the removal of toxic materials such as chemotherapeutic drugs from cells, increased intercellular communication, or a modulation of the microenvironment for migration, immune regulation, or cancer metastasis [6, 29, 31]. Patients in our good prognostic group exhibited increased EV concentrations after treatment with methotrexate. A possible explanation could be the different mechanisms of action between drugs, such as cisplatin and adriamycin (doxorubicin) must be eliminated by dealkylating or DNA repair enzymes, whereas

methotrexate is an anti-metabolite. Another possible explanation is that our observed EVs may include not only exosomes but also microvesicles and apoptotic bodies. Thus, increased EV concentrations after treatment might reflect cellular stress and early apoptosis[26].

Unfortunately, we could not separate exosomes, microvesicles and apoptotic bodies in this study. However, the decreased EV concentration in this study was proved to reflect decreased concentration of exosome surface marker bearing EVs by both MACSPlex APC-conjugate beads and ExoView Tetraspanin Chips. We evaluated the implications of changes in EV concentration in a discrete cohort of LM patients with the same primary cancer of NSCLC, adenocarcinoma who underwent the same protocol of phase II ventriculolumbar perfusion methotrexate chemotherapy. The prognostic value of miR-21 in NSCLC patients has been examined in many studies [32–35]. Our finding of markedly elevated miR-21 expression in patients with poor overall survival (and decreased EV concentration) and decreased miR-21 expression in patients with better overall survival (and increased EV concentration) after intravascular CSF chemotherapy is consistent with previous studies. Furthermore, our miR-21 data were obtained from a prospective clinical trial in which LM patients had the same primary cancer of NSCLC and received the same designated treatment protocol, proven CSF cytology, and times of CSF sampling (days 0 and 4). Thus, the prognostic meaning of miR-21 expression levels in paired samples is more valuable than that which could be obtained through spot sampling or primary cancer-only studies.

It remains technical problem of evaluating CSF microRNA expression level due to both the absence of endogenous control for normalization and the origin of microRNA (exosomal vs. non-exosomal) [11, 12]. Recently, Parieto-Fernandez et al. performed a comprehensive measurement of CSF microRNA differentiating vesicular from non-vesicular compartment [36]. According to their study, miR-21 existed mainly in non-vesicular (CD63 negative) fraction and was nearly abolished with proteinase and RNase combined treatment. In our study, we did not use EV enrichment procedure such as ultracentrifugation or chromatography but extract RNA from cleared CSF. Thus, our CSF samples naturally include non-vesicular microRNA. However, we could not explain why the miR-21 expression pattern became significantly different between EV-decreased and EV-increased groups not by RNA amount but by NTA-measure EV concentration at this study design. Very low concentration of CSF extracellular RNA may give inconsistent results according to different extraction and RT-PCR methods [36, 37]. We expect more sophisticated EV extraction method keeping non-vesicular proteins and microRNAs from undesirable loss or damage and solid standard RNA extraction and RT-PCR process could help to solve this question in future.

In this study, we also tracked changes in EV concentration and miR-21 expression in the CSF of LM patients after the intraventricular chemotherapy. Decreased post-treatment EV concentration and increased miR-21 expression was associated with poor prognosis in NSCLC patients with LM, who underwent intra-CSF methotrexate chemotherapy. We believe that our observation could be used as reference values for future CSF nanoparticle study and developed as a method in clinical practice to monitor treatment response in these patients with LM.

# Conclusions

Extracellular vesicles (EVs) in biofluids are recently studied for their distribution, concentration, and contents to monitor disease status especially in cancer. Here, we measured nanoparticles in human CSF from 472 controls and patients including leptomeningeal metastasis (LM), which has neither effective treatment nor biomarkers for disease progression or treatment response by both Dynamic Light Scattering and Nanopaticle Tracking Analysis with a minimal manipulation of two-step centrifugation. Then, we analyzed the difference of size and concentration according to different CNS disease status. And also, we found the change of EVs concentration after intra-CSF chemotherapy in patients with LM to correlate with patients overall survival, and the expression level of onco-microRNA (miR-21) was in inverse proportion to EV concentration change in non-small cell lung cancer. Our measurement of combined EVs

concentration and onco-miR for LM chemotherapy could be performed in moderately equipped institution, and help physicians to monitor this possible neurotoxic treatment.

# List Of Abbreviations

EVs, Extracellular vesicles; LM, leptomeningeal metastasis; DLS, Dynamic Light Scattering; NTA, and Nanoparticle Tracking Analysis; CSF, Cerebrospinal fluid; CNS, central nervous system; MFI, fluorescence intensity; ddPCR, digital droplet polymerase chain reaction; NSCLC, Non-small cell lung cancer; PSD, particle size distribution; SD, standard deviation; VLP, ventriculolumbar perfusion; ANOVA, analysis of variance; CI, confidence interval; OS, overall survival

# Declarations

### Ethics approval and consent to participate

This observational study was approved by the Institutional Review Board of the National Cancer Center (NCC-150002, NCC-2014-0135), followed all rules and regulations regarding the protection of human subjects in clinical research, and in accordance with the ethical guidelines outlined in the Declaration of Helsinki. All patients were signed informed consent.

### Consent for publication

Not applicable

### Availability of data and materials

The datasets used and/or analysed during the current study are available from the corresponding author on reasonable request.

### Competing interests

All authors declare that no conflict of interest exists.


### Funding

This work was supported by the National Cancer Center under Grant 1710871-3 and 1910090-1; the Ministry of Health and Welfare, Republic of Korea under Grant H17C1018


### Authors contributions

H-S.G, JH.K, BC.Y, JB.P, and H-J.K designed and supervised the study. H-S.G, HJ.P, H-J.K, JW.K, SH.S, and H.Y collected human CSF samples and determined diagnosis of CNS diseases. K-Y.L, JH.I, W.L, TH.K, and C.L performed experiments and analysed data. H-S.G, K-Y.L, JH.I, and C.L constructed the manuscript. All authors revised and approved the manuscript.


## Acknowledgements

We thank Jeong Eun Kim (Seoul National University Medical College), Chae Hyuk Lee (Inje Medical University), and Seung Yeop Yang (Donguk Medical University) for assistance with CSF collection.


# References

1. O.M. Debus, A. Lerchl, H.W. Bothe, J. Bremer, B. Fiedler, M. Franssen, J. Koehring, M. Steils, G. Kurlemann, Spontaneous central melatonin secretion and resorption kinetics of exogenous melatonin: a ventricular CSF study, J Pineal Res, 33 (2002) 213-217.
2. S.V. Frankfort, L.R. Tulner, J.P. van Campen, M.M. Verbeek, R.W. Jansen, J.H. Beijnen, Amyloid beta protein and tau in cerebrospinal fluid and plasma as biomarkers for dementia: a review of recent literature, Curr Clin Pharmacol, 3 (2008) 123-131.
3. M.J. Romeo, V. Espina, M. Lowenthal, B.H. Espina, E.F. Petricoin, 3rd, L.A. Liotta, CSF proteome: a protein repository for potential biomarker identification, Expert Rev Proteomics, 2 (2005) 57-70.
4. J.W. Hyun, J.H. Park, B.G. Kang, E.Y. Park, B. Park, J. Joo, J.K. Kim, S.H. Kim, J.H. Jeong, H.W. Lee, K.D. Park, K.G. Choi, S.H. Hwang, H.S. Gwak, H.J. Kim, Diagnostic and prognostic values of cerebrospinal fluid CYFRA 21-1 in patients with leptomeningeal carcinomatosis, Oncotarget, 8 (2017) 53326-53335.
5. B. Gyorgy, T.G. Szabo, M. Pasztoi, Z. Pal, P. Misjak, B. Aradi, V. Laszlo, E. Pallinger, E. Pap, A. Kittel, G. Nagy, A. Falus, E.I. Buzas, Membrane vesicles, current state-of-the-art: emerging role of extracellular vesicles, Cell Mol Life Sci, 68 (2011) 2667-2688.
6. D.D. Gonda, J.C. Akers, R. Kim, S.N. Kalkanis, F.H. Hochberg, C.C. Chen, B.S. Carter, Neuro-oncologic applications of exosomes, microvesicles, and other nano-sized extracellular particles, Neurosurgery, 72 (2013) 501-510.
7. M.G. Harrington, A.N. Fonteh, E. Oborina, P. Liao, R.P. Cowan, G. McComb, J.N. Chavez, J. Rush, R.G. Biringer, A.F. Huhmer, The morphology and biochemistry of nanostructures provide evidence for synthesis and signaling functions in human cerebrospinal fluid, Cerebrospinal Fluid Res, 6 (2009) 10.
8. J.M. Street, P.E. Barran, C.L. Mackay, S. Weidt, C. Balmforth, T.S. Walsh, R.T. Chalmers, D.J. Webb, J.W. Dear, Identification and proteomic profiling of exosomes in human cerebrospinal fluid, J Transl Med, 10 (2012) 5.
9. N.M. Teplyuk, B. Mollenhauer, G. Gabriely, A. Giese, E. Kim, M. Smolsky, R.Y. Kim, M.G. Saria, S. Pastorino, S. Kesari, A.M. Krichevsky, MicroRNAs in cerebrospinal fluid identify glioblastoma and metastatic brain cancers and reflect disease activity, Neuro Oncol, 14 (2012) 689-700.
10. J.C. Akers, V. Ramakrishnan, J.P. Nolan, E. Duggan, C.C. Fu, F.H. Hochberg, C.C. Chen, B.S. Carter, Comparative Analysis of Technologies for Quantifying Extracellular Vesicles (EVs) in Clinical Cerebrospinal Fluids (CSF), PLoS One, 11 (2016) e0149866.
11. K.L. Burgos, A. Javaherian, R. Bomprezzi, L. Ghaffari, S. Rhodes, A. Courtright, W. Tembe, S. Kim, R. Metpally, K. Van Keuren-Jensen, Identification of extracellular miRNA in human cerebrospinal fluid by next-generation sequencing, Rna, 19 (2013) 712-722.
12. Y. Yagi, T. Ohkubo, H. Kawaji, A. Machida, H. Miyata, S. Goda, S. Roy, Y. Hayashizaki, H. Suzuki, T. Yokota, Next-generation sequencing-based small RNA profiling of cerebrospinal fluid exosomes, Neurosci Lett, 636 (2017) 48-57.
13. M.C. Chamberlain, Leptomeningeal metastases: a review of evaluation and treatment, J Neurooncol, 37 (1998) 271-284.
14. W. Boogerd, M.J. van den Bent, P.J. Koehler, J.J. Heimans, J.J. van der Sande, N.K. Aaronson, A.A. Hart, J. Benraadt, J. Vecht Ch, The relevance of intraventricular chemotherapy for leptomeningeal metastasis in breast cancer: a randomised study, Eur J Cancer, 40 (2004) 2726-2733.
15. R.J. Freilich, G. Krol, L.M. DeAngelis, Neuroimaging and cerebrospinal fluid cytology in the diagnosis of leptomeningeal metastasis, Ann Neurol, 38 (1995) 51-57.
16. M.J. Glantz, B.F. Cole, L.K. Glantz, J. Cobb, P. Mills, A. Lekos, B.C. Walters, L.D. Recht, Cerebrospinal fluid cytology in patients with cancer: minimizing false-negative results, Cancer, 82 (1998) 733-739.
17. M. Chamberlain, L. Junck, D. Brandsma, R. Soffietti, R. Ruda, J. Raizer, W. Boogerd, S. Taillibert, M.D. Groves, E. Le Rhun, J. Walker, M. van den Bent, P.Y. Wen, K.A. Jaeckle, Leptomeningeal metastases: a RANO proposal for

response criteria, Neuro Oncol, 19 (2017) 484-492.

18. M.C. Chamberlain, Cytologically negative carcinomatous meningitis: usefulness of CSF biochemical markers, Neurology, 50 (1998) 1173-1175.
19. M.C. Chamberlain, P. Kormanik, Carcinoma meningitis secondary to non-small cell lung cancer: combined modality therapy, Arch Neurol, 55 (1998) 506-512.
20. H.S. Gwak, J. Joo, S. Kim, H. Yoo, S.H. Shin, J.Y. Han, H.T. Kim, J.S. Lee, S.H. Lee, Analysis of treatment outcomes of intraventricular chemotherapy in 105 patients for leptomeningeal carcinomatosis from non-small-cell lung cancer, J Thorac Oncol, 8 (2013) 599-605.
21. O.P.B. Wiklander, R.B. Bostancioglu, J.A. Welsh, A.M. Zickler, F. Murke, G. Corso, U. Felldin, D.W. Hagey, B. Evertsson, X.M. Liang, M.O. Gustafsson, D.K. Mohammad, C. Wiek, H. Hanenberg, M. Bremer, D. Gupta, M. Bjornstedt, B. Giebel, J.Z. Nordin, J.C. Jones, S. El Andaloussi, A. Gorgens, Systematic Methodological Evaluation of a Multiplex Bead-Based Flow Cytometry Assay for Detection of Extracellular Vesicle Surface Signatures, Front Immunol, 9 (2018) 1326.
22. D. Bachurski, M. Schuldner, P.H. Nguyen, A. Malz, K.S. Reiners, P.C. Grenzi, F. Babatz, A.C. Schauss, H.P. Hansen, M. Hallek, E. Pogge von Strandmann, Extracellular vesicle measurements with nanoparticle tracking analysis - An accuracy and repeatability comparison between NanoSight NS300 and ZetaView, J Extracell Vesicles, 8 (2019) 1596016.
23. Y. Shim, H.S. Gwak, S. Kim, J. Joo, S.H. Shin, H. Yoo, Retrospective Analysis of Cerebrospinal Fluid Profiles in 228 Patients with Leptomeningeal Carcinomatosis : Differences According to the Sampling Site, Symptoms, and Systemic Factors, J Korean Neurosurg Soc, 59 (2016) 570-576.
24. H.S. Gwak, J. Joo, S.H. Shin, H. Yoo, J.Y. Han, H.T. Kim, T. Yun, J. Ro, J.S. Lee, S.H. Lee, Ventriculolumbar perfusion chemotherapy with methotrexate for treating leptomeningeal carcinomatosis: a Phase II Study, Oncologist, 19 (2014) 1044-1045.
25. Y. Gui, H. Liu, L. Zhang, W. Lv, X. Hu, Altered microRNA profiles in cerebrospinal fluid exosome in Parkinson disease and Alzheimer disease, Oncotarget, 6 (2015) 37043-37053.
26. J.C. Akers, D. Gonda, R. Kim, B.S. Carter, C.C. Chen, Biogenesis of extracellular vesicles (EV): exosomes, microvesicles, retrovirus-like vesicles, and apoptotic bodies, J Neurooncol, 113 (2013) 1-11.
27. D. Bartczak, P. Vincent, H. Goenaga-Infante, Determination of size- and number-based concentration of silica nanoparticles in a complex biological matrix by online techniques, Anal Chem, 87 (2015) 5482-5485.
28. K. Al-Nedawi, B. Meehan, J. Micallef, V. Lhotak, L. May, A. Guha, J. Rak, Intercellular transfer of the oncogenic receptor EGFRvIII by microvesicles derived from tumour cells, Nat Cell Biol, 10 (2008) 619-624.
29. K. Shedden, X.T. Xie, P. Chandaroy, Y.T. Chang, G.R. Rosania, Expulsion of small molecules in vesicles shed by cancer cells: association with gene expression and chemosensitivity profiles, Cancer Res, 63 (2003) 4331-4337.
30. R. Spaull, B. McPherson, A. Gialeli, A. Clayton, J. Uney, A. Heep, O. Cordero-Llana, Exosomes populate the cerebrospinal fluid of preterm infants with post-haemorrhagic hydrocephalus, Int J Dev Neurosci, 73 (2019) 59-65.
31. R. Safaei, B.J. Larson, T.C. Cheng, M.A. Gibson, S. Otani, W. Naerdemann, S.B. Howell, Abnormal lysosomal trafficking and enhanced exosomal export of cisplatin in drug-resistant human ovarian carcinoma cells, Mol Cancer Ther, 4 (2005) 1595-1604.
32. W. Zheng, J. Zhao, Y. Tao, M. Guo, Z. Ya, C. Chen, N. Qin, J. Zheng, J. Luo, L. Xu, MicroRNA-21: A promising biomarker for the prognosis and diagnosis of non-small cell lung cancer, Oncol Lett, 16 (2018) 2777-2782.
33. Y. Yuan, X.Y. Xu, H.G. Zheng, B.J. Hua, Elevated miR-21 is associated with poor prognosis in non-small cell lung cancer: a systematic review and meta-analysis, Eur Rev Med Pharmacol Sci, 22 (2018) 4166-4180.
34. L.E. Buscaglia, Y. Li, Apoptosis and the target genes of microRNA-21, Chin J Cancer, 30 (2011) 371-380.

35. L. Xu, Y. Huang, D. Chen, J. He, W. Zhu, Y. Zhang, X. Liu, Downregulation of miR-21 increases cisplatin sensitivity of non-small-cell lung cancer, Cancer Genet, 207 (2014) 214-220.
36. E. Prieto-Fernandez, A.M. Aransay, F. Royo, E. Gonzalez, J.J. Lozano, B. Santos-Zorrozua, N. Macias-Camara, M. Gonzalez, R.P. Garay, J. Benito, A. Garcia-Orad, J.M. Falcon-Perez, A Comprehensive Study of Vesicular and Non-Vesicular miRNAs from a Volume of Cerebrospinal Fluid Compatible with Clinical Practice, Theranostics, 9 (2019) 4567-4579.
37. J.A. Saugstad, T.A. Lusardi, K.R. Van Keuren-Jensen, J.I. Phillips, B. Lind, C.A. Harrington, T.J. McFarland, A.L. Courtright, R.A. Reiman, A.S. Yeri, M.Y.S. Kalani, P.D. Adelson, J. Arango, J.P. Nolan, E. Duggan, K. Messer, J.C. Akers, D.R. Galasko, J.F. Quinn, B.S. Carter, F.H. Hochberg, Analysis of extracellular RNA in cerebrospinal fluid, J Extracell Vesicles, 6 (2017) 1317577.

## Figures

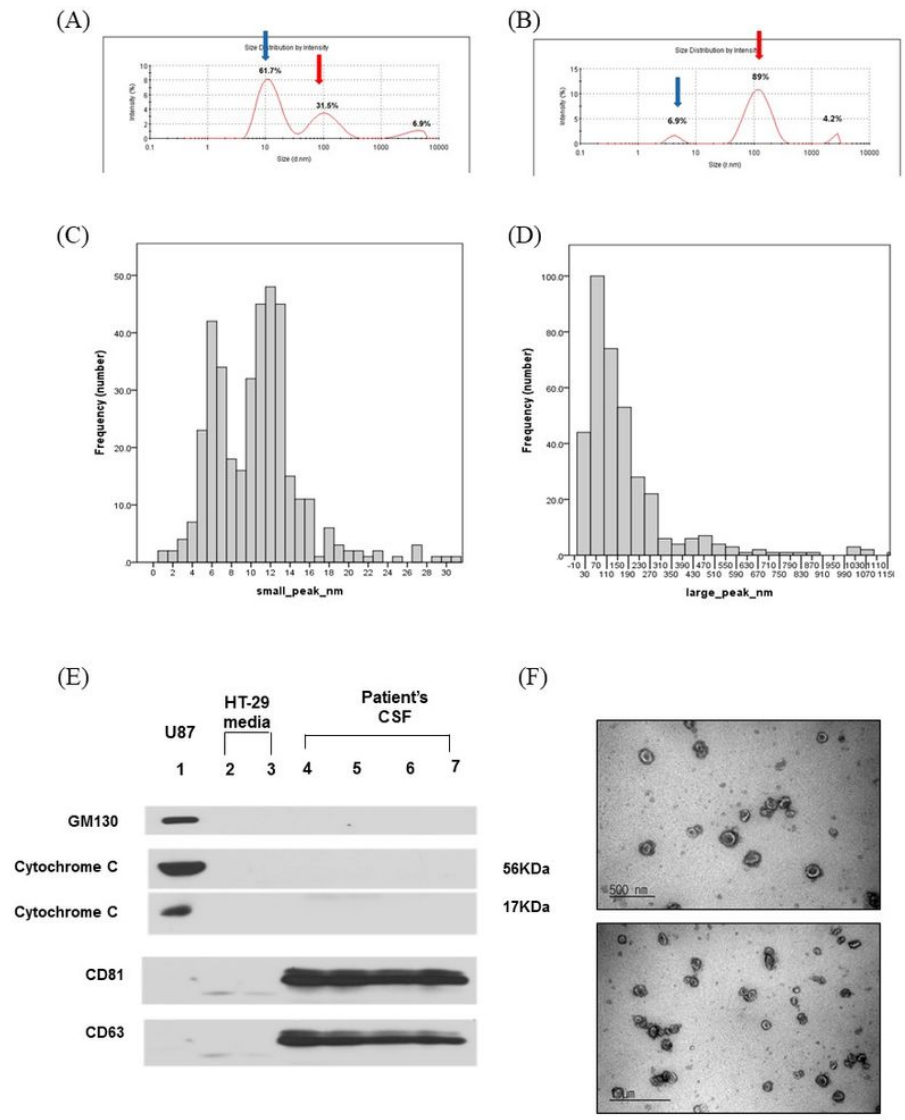


## Figure 1

Identification of extracellular vesicle markers from CSF. (A and B) Representative diagram of observed peaks of nano-particles in human cerebrospinal fluid by Dynamic Light Scattering (DLS) using Zetasizer Nano system. (A) healthy control and (B) leptomeningeal metastasis (LM). (C and D) Histogram depicting the two peaks in human CSF (n=472) observed by Dynamic Light Scattering (DLS) using Zetasizer Nano system. (C) The small peak was measured at a mean 10.5 nm and (D) the large peak was observed at a mean of 176 nm. (E) Western blot of human CSF for exosomal markers. Upper 3 rows are cytosolic marker (GM 130 and Cytochrome c) and U87 glioma cell extract was used as positive control. Lower 2 rows represent exosomal membrane protein (CD81 and CD3) and HT-29 cell culture supernatant was for positive control of exosome. (F) Transmission Electron Microscopy showing bi-membranous vesicles of purified CSF exosomes.

Figure 2

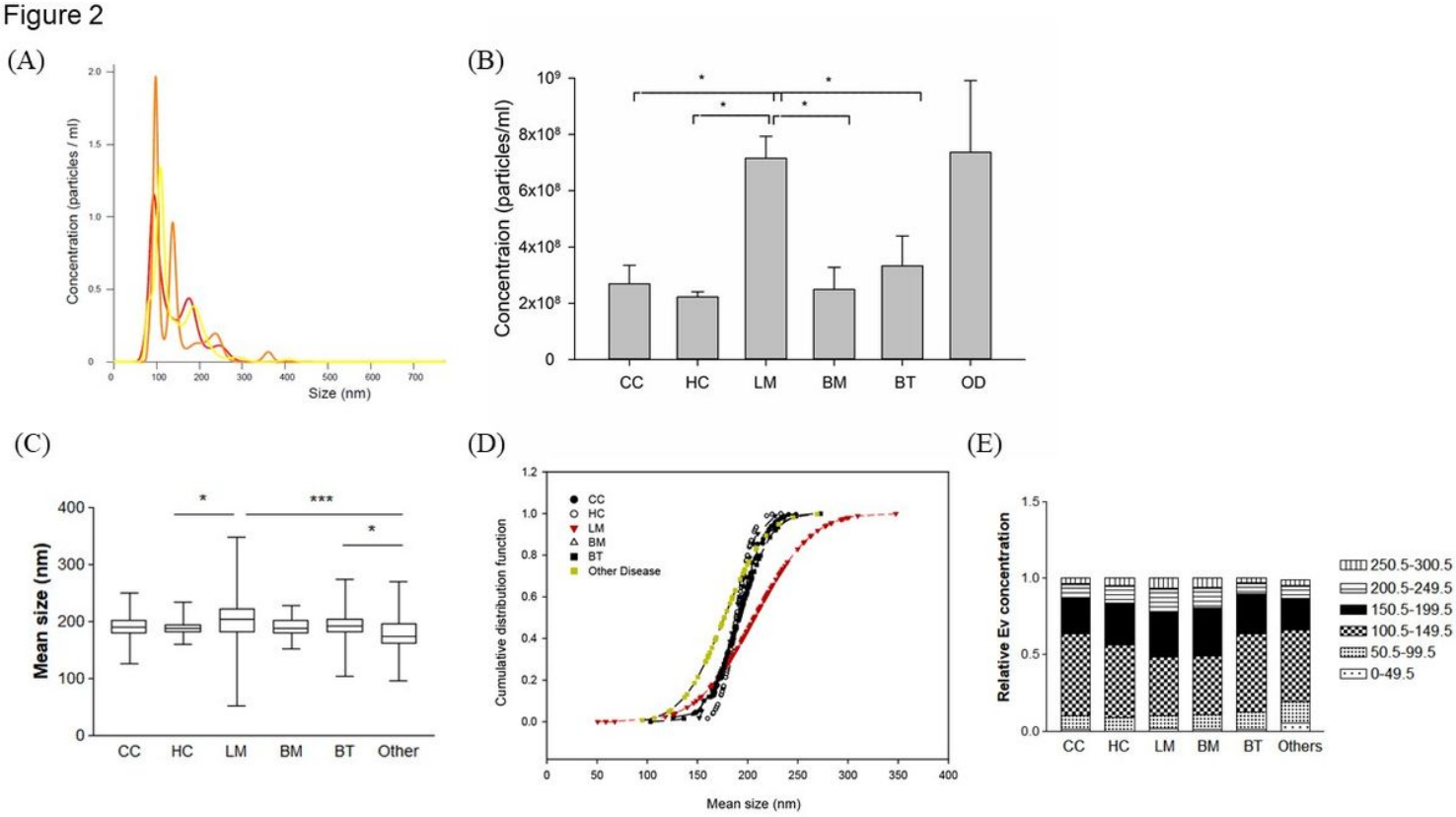


## Figure 2

The number of extracellular vesicles (EV) measured by Nanoparticle Tracking Analysis using Nanosight NS300 system according to patients groups. (A) Representative image of NTA measurement (repeated 3 times per one sample and an average value was provided). (B) EV concentration according to patients groups. Different EV concentration among group of 'Other disease' according to different disease of multiple sclerosis, intracranial hemorrhage and CNS infection (see details in Supplementary figure 4) (ANOVA, Dunn's Multiple Comparison, *p<0.05). (C) Box plot of size distribution of EV according to patients groups. The thick bar represents mean value and the box denote quartile range. (ANOVA, Dunn's Multiple Comparison, *p<0.05, ***p<0.001) (D) Empirical cumulative distribution plot of mean size of extracellular vesicles. (ECDF were generated by the Ecdf function in R, Kolmogorov–Smirnov test were performed to compare the significance between groups) (E) The proportion of EV size by tentative size interval of 50 nm (0-300 nm). Abbreviations: CC, cancer control; HC, healthy control; LM, leptomeningeal metastasis; BM, brain metastasis; BT, brain tumor.

Figure 3

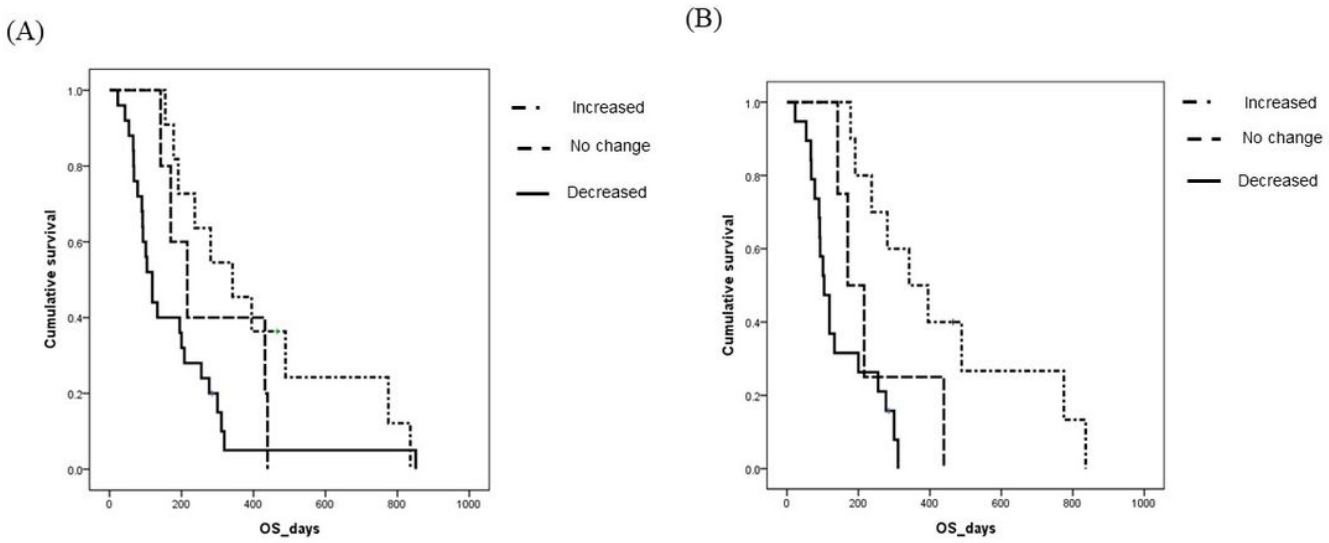


## Figure 3

Kaplan-Meier overall survival analysis of patients who received the same intra-CSF chemotherapy for LM according to the extracellular vesicle concentration change after the treatment. (A) all 41 patients with various primary cancer (p=0.037), and (B) non-small cell lung cancer patients (n=33, p < 0.001).

Figure 4

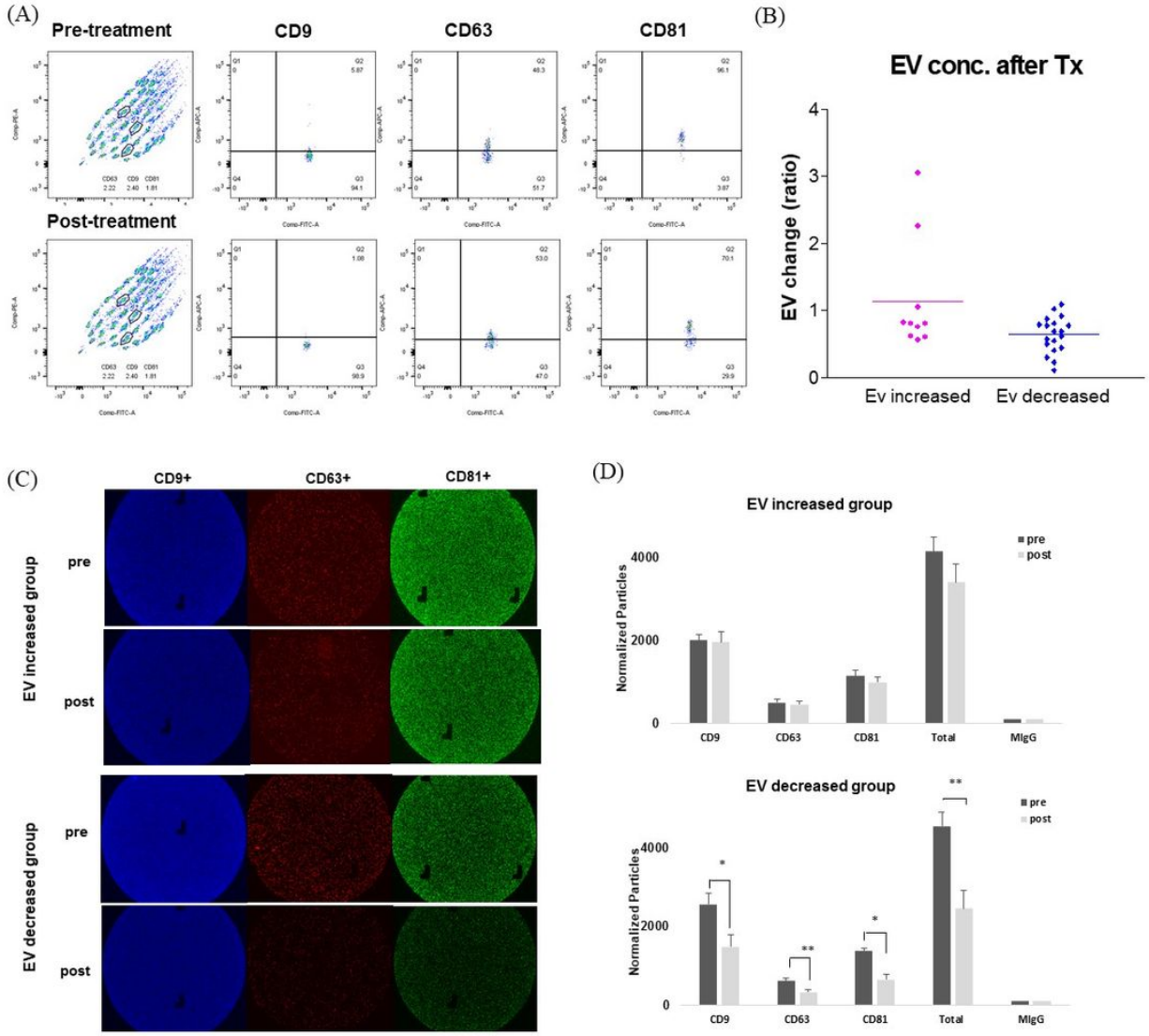


## Figure 4

Evaluation of exosome concentration change after intraventricular chemotherapy by surface markers. (A) flow cytometry using the MACSPlex Exosome Kit. (B) The relative expression of EV markers was determined by the mean fluorescence intensity (MFI) of APC-conjugated capture antibody. In the EV decreased group, the exosome markers were significantly reduced after intraventricular chemotherapy (ratio 0.64, $p < 0.001$), whereas increased groups showed no significant exosome concentration change (ratio 1.13). (C) ExoView Tetraspanin Chip revealing exosome surface markers (CD9 in red, CD63 in green and CD81 in blue). (D) The change of each exosome markers after the intraventricular chemotherapy showed significant decrease of all exosome markers in EV decreased groups ($p^{*}<0.05$, $p^{**}<0.005$). Tx: Treatment.

Figure 5

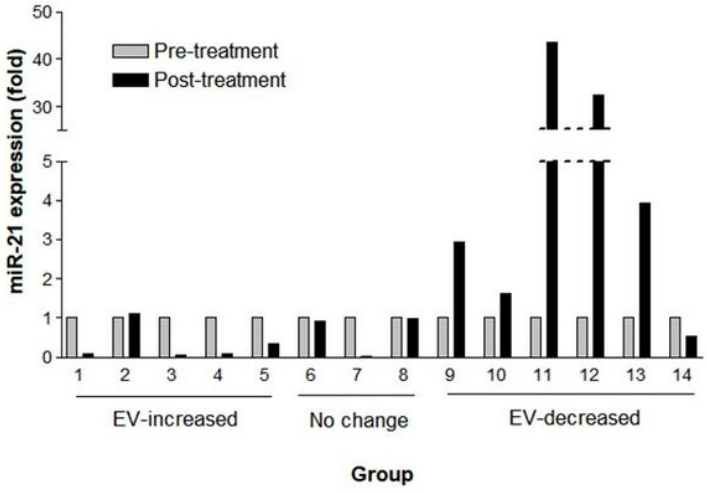


**Figure 5**

Fold change of miR-21 expression by digital droplet PCR paired pre-treatment (gray column) and post-treatment (black column) CSF samples according to EV changes of increased (n=5), 'no change' (n=3), and decreased (n=6) EV concentration after the intraventricular chemotherapy. CSF extracellular miR-21 was detected by digital droplet PCR and normalized with EV concentration.

## Supplementary Files

This is a list of supplementary files associated with this preprint. Click to download.

- SupplementaryTables.docx
- SupplementaryTables.docx
- SupplementaryTables.docx
- SupplementaryFigure1.pdf
- SupplementaryFigure1.pdf
- SupplementaryFigure1.pdf